

Mouse macrophage metalloelastase generates angiostatin from plasminogen and suppresses tumor angiogenesis in murine colon cancer

ZHANGWEI XU^{1,2,3}, HAI SHI¹, QI LI⁴, QIAO MEI¹,
JUNJUN BAO³, YUXIAN SHEN⁴ and JIANMING XU^{1,3}

Departments of ¹Gastroenterology, ²Geriatrics, the First Affiliated Hospital, Anhui Medical University, Hefei 230022, Anhui Province; ³The Key Laboratory of Gastroenterology of Anhui Province; ⁴The Key Laboratory of Gene Resource Utilization for Genetic Diseases, Ministry of Education and Anhui Province, Hefei 230032, P.R. China

Received January 31, 2008; Accepted April 4, 2008

Abstract. Previous studies showed that the mouse macrophage metalloelastase (MME) generates the angiogenesis inhibitor angiostatin from plasminogen *in vitro*. This study aimed to determine whether tumor cells engineered with MME could generate angiostatin and suppress tumor angiogenesis *in vivo*. Murine CT-26 colon cancer cells stably transfected with MME were inoculated subcutaneously. A radioisotope tracer, immunoblotting, immunofluorescence and immunohistochemistry were used to explore the pathway of the angiostatin generation. The results showed that tumors derived from MME-transfected cells demonstrated a less microvessel density compared with control tumors derived from vector-transfected and non-transfected cells ($P < 0.001$). The expression of vascular endothelial growth factor (VEGF) was significantly lower in the MME-transfected group compared with that of the controls. The growth of MME-transfected tumors was significantly retarded compared with the control tumors ($P < 0.001$). Western blot analysis, using a specific anti-mouse plasminogen (1-4 Kringle) antibody, demonstrated two strong immunoreactive bands (38- and 35-kDa) in MME-transfected tumors. γ -ray counting data demonstrated that plasminogen cleavage occurred mostly in tumors formed by cells forced to express. We concluded that MME was demonstrated to be an efficient angiostatin-producing MMP and its presence was negatively correlated with the growth of colon cancer in tumor-bearing mice. These findings provide direct evidence that MME generates angiostatin in tumor-bearing mice and the therapeutic application of MME against tumors.

Introduction

Tumor-associated proteases are suggested to play a crucial role in tumor invasion and angiogenesis in a variety of malignancies (1,2). Colorectal carcinoma is one of the important malignant tumors of the digestive system, but there has been very limited research on the proteolytic activity of matrix metalloproteinase (MMP) in the growth and metastasis of colon cancer.

MME, a member of the MMP family, was first detected in mouse peritoneal macrophage-conditioned media in 1975 (3). This enzyme has a broad substrate specificity for matrix macromolecules (4). It was found that the forced expression of MME is capable of suppressing the growth and angiogenesis of murine melanoma (5). Additionally, Dong *et al* (6) demonstrated the role of MME in converting plasminogen into angiostatin *in vitro*. In hepatocellular carcinoma, the expression of MME has been associated with angiostatin production and a favorable outcome (7), but the reverse has been reported in dermal squamous cell and non-small cell lung carcinomas (8,9). The exact role of MME in the generation of angiostatin during the macrophage infiltration of a tumor and its influence on colon cancer growth remain unclear.

To better understand the role of MME in the generation of angiostatin and the inhibition of colon tumor angiogenesis, we transfected the MME gene into murine colon cancer cells and studied its anti-tumor and anti-angiogenic activities in a subcutaneously implanted tumor model. Moreover, we show the generation of angiostatin from plasminogen in mice-bearing MME-transfected tumors using isotope tracers and Western blot analysis.

Materials and methods

Construction of the GFP-tagged recombinant plasmid. The construction of recombinant MME in pcDNA3.1 has been reported by our research group (10). To generate a GFP-tagged MME, pcDNA3.1-MME and pEGFP-C1 (Clontech, USA) were cut with *Xba*I and *Bam*HI (Takara, Dalian, P.R. China),

Correspondence to: Dr Jianming Xu, Department of Gastroenterology, the First Affiliated Hospital, Anhui Medical University, Hefei 230022, Anhui Province, P.R. China
E-mail: xzw2jj2005@yahoo.com.cn

Key words: mouse macrophage metalloelastase, tumor angiogenesis, angiostatin, animal model, colon carcinoma

and MME was inserted into the green fluorescent fusion expression vector pEGFP-C1 between the *Xba*I and *Bam*HI sites. The expression unit was confirmed by sequencing (Songon Co., Shanghai, P.R. China).

Cell line culture and transfection. The murine colon carcinoma cell line CT-26 was obtained from Dr Huoye Gan (the Molecular Center, Second Affiliated Hospital, Guangzhou Medical College, P.R. China). The cells were cultured in Dulbecco's modified Eagle's medium (DMEM, Gibco BRL, USA) supplemented with 10% heat-inactivated fetal calf serum (FCS) and maintained in humidified 95% air and 5% CO₂ at 37°C. The cells were split into 6-well dishes 24 h before transfection and transfected at 70-80% confluence using Lipofectamine 2000 (Invitrogen, USA) according to the manufacturer's instructions. Cells transfected with the empty vector (pEGFP-C1) were used as controls. The cells were selected for 3 weeks in a medium containing G418 (800 µg/ml, Sangon Biotechnology, Inc., P.R. China) to derive cell lines stably expressing MME (CT-26-MME-GFP) and CT-26-GFP (control). Individual colonies were chosen after 3 weeks of culture and used for further investigation. The transfected cells were maintained in a medium containing 200 µg/ml G418.

In vitro assay of MME on CT-26 cell growth. Stable MME-, vector- and non-transfected CT-26 cells were plated in 96-well plates at a density of 5x10³ cells per well 24-72 h after transfection. Cell viability was measured by a 3-(4,5-dimethylthiazol-2-yl)-2,5-diphenyltetrazolium bromide (MTT, Sigma, USA) reduction as described (11). MTT was dissolved at a concentration of 5 mg/ml in sterile PBS. Following a total of 72 h of treatment, 25 µl of the 5 mg/ml solution of MTT were added to each well, and the incubation continued for 3 h. Then 100 µl of the cell lysis buffer (20% SDS/50% N,N-dimethylformamide, pH 4.7) were added. The absorbance was read at 570 nm on a microplate reader (Camberra Packard, MI, IT). To assess cell viability, cell counts using trypan blue exclusion were also performed.

Western blot analysis. Plasmids were transiently transfected into CT-26 cells. The cells were harvested 24-30 h after transfection and lysed in 2% SDS sample buffer, followed by SDS-PAGE analysis. The proteins were then transferred to PVDF membranes and blocked with 5% non-fat dried milk in PBS with 0.1% Tween-20 for 30 min at room temperature. Primary antibodies (dilution 1:250, goat anti-mouse MME, Santa Cruz Biotechnology, Santa Cruz, USA) were diluted in 5% milk and incubations were carried out at 4°C overnight. HRP-conjugated anti-goat IgG were used as secondary antibodies. Blots were developed using the enhanced chemiluminescence (ECL) detection system (Amersham Biosciences, UK). The level of protein expression by Western blot analysis was quantified by image analysis using the Bio-Rad Quantity One system. All the results are derived from three to four separate experiments.

Gelatin zymography analysis. CT-26 cells transfected with MME-, vector- and non-transfected cells, were cultured in DMEM without FCS for 24 h and collected at 80% confluence.

The cells were then lysed by sonication. After centrifugation at 15,000 rpm for 20 min, the supernatants were collected and mixed with non-reducing sample buffer without boiling. They were subjected to electrophoresis in 10% SDS-PAGE gel impregnated with 2 mg/Fml gelatin (Sigma, St. Louis, MO, USA) under non-denaturing conditions. The amount of protein applied to the gel was 40 µg. After electrophoresis, SDS was eluted from the gel by washing in 2.5% Triton X-100 for 30 min to allow the proteins to re-nature. The gel was then incubated at 37°C for 18 h in substrate buffer (0.05 M Tris-HCl, pH 8.0, 5 mM CaCl₂, 0.15 M NaCl) and stained with 0.1% Coomassie brilliant blue R-250. Gelatin-degrading activity was indicated by the appearance of clear bands against a blue background.

Preparation of radioiodine-labeled plasminogen. Mouse plasminogen (Pharmacia, Uppsala, Sweden) was dissolved in distilled water, aliquoted and stored at -70°C until use. The plasminogen was radioiodine-labeled using the chloramine-T method described previously (12). Briefly, 30 µg of plasminogen was labeled with ~1.5 mCi of Na¹²⁵I (Amersham Pharmacia, Buckinghamshire, UK) and 50 µg of chloramine-T (Sigma, USA) in 20 mM phosphate buffer (pH 7.2) in a final volume of 110 µl. Iodination was allowed to proceed at 4°C for 1 min. The reaction was terminated upon the addition of 5 µl of sodium metabisulfite (5 mg/ml). The ¹²⁵I-plasminogen was purified on a gel filtration (Sephadex G-25) column (Amersham Biosciences, Uppsala, Sweden) with 0.01 N PBS passed at 1 ml/5min through the column. The radioactivity of samples from each fraction was measured with a γ counter, and the fraction from the first activity peak was diluted in PBS (pH 7.4) and used for experiments. The ¹²⁵I-plasminogen displayed specific activities that ranged from 24 to 34 µCi/mg of plasminogen.

Subcutaneously implanted tumor model studies. Specific pathogen-free female Balb/c mice (6-week-old) were purchased from Sino-British SIPPR/BK Lab Animal Ltd. (Shanghai, P.R. China). Mice were fed on standard mouse food. Potassium iodide (KI, 2 mg/kg body weight) was orally administered twice daily to block the uptake of ¹²⁵I-plasminogen by the thyroid. Control or MME-transfected CT-26 cells in the exponential growth phase were harvested by a brief exposure to 0.25% trypsin solution. The cell suspensions were pipetted to produce a single-cell suspension. The cell viability was determined by trypan blue, and only single-cell suspensions of >90% viability were used. Solid tumors (n=30 mice for each group) were produced by the intradermal injection of 5x10⁵ viable cells (in 50 µl of DMEM) into the alar skin. The tumor volume of each mouse, calculated using the formula (13): smallest diameter x widest diameter/2, was measured daily using calipers after the mice had been anesthetized with ether. Mice were euthanized after 4 weeks or when they became moribund. Tumors were excised, fixed in 4% paraformaldehyde 0.1 M PBS containing 0.1% diethyl pyrocarbonate (DEPC), and embedded in paraffin according to standard histological procedures. For *in vivo* biodistribution studies, tumor-bearing mice were injected via the tail vein with 1-5 µCi of ¹²⁵I-plasminogen and sacrificed at 72 h after injection (14,15). Blood, major organs and tumor tissue were

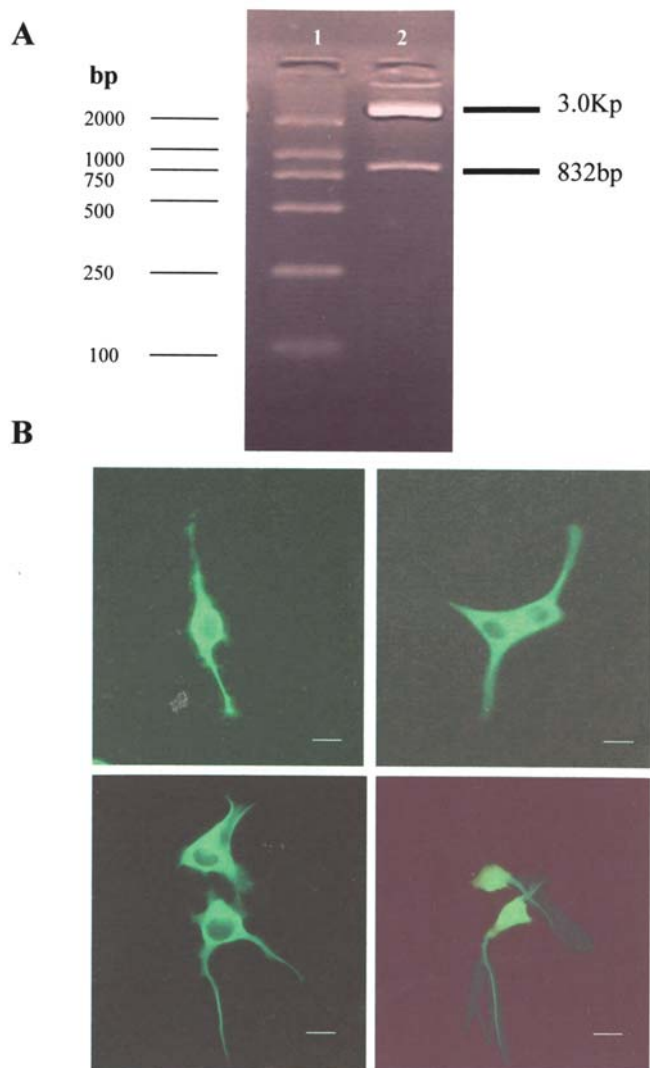


Figure 1. Identification and transfection of the recombinant plasmid. (A) Identification of the expression vector pEGFP-C1-MME. Lane 1: DL 2000 marker. Lane 2: products of the expression vector pEGFP-C1-MME digested by *Bam*HI and *Xba*I (~5.4 kb and 832 bp, respectively) with 1% agarose gel electrophoresis. (B) Observed under the fluorescent microscopy after stable transfection. It shows CT-26 cell division and proliferation after stable transfection and GFP location of the cytoplasm or distribution of the whole cell. Bar inset, 20 μ m; original magnification, x400.

promptly excised, weighed and measured (5). All of the animal experiments were performed in compliance with the Guide for the Care and Use of Laboratory Animals of Anhui Medical University.

SDS-PAGE electrophoresis and γ -ray counting analysis (16). The SDS-PAGE electrophoresis was carried out as described above. After electrophoresis, the gels were stained in at least five volumes of staining solution containing 0.25% Coomassie brilliant blue in methanol, H₂O and glacial acetic acid (45/45/10 v/v/v) and placed on a slowly rotating platform for 4 h at room temperature. The staining solution was then removed and the gel was destained by soaking it in a solution of methanol, H₂O and acetic acid (45:45:10 v/v/v) without the dye on a slowly rocking platform for 6 h. The destaining solution was changed every 2 h. The gels were photographed

and the stained protein bands were cut out for subsequent analysis.

The 35 and 38 kDa from each lane were excised and placed in a measuring buret, which contained the weakly stained band plus the stacking gel. These fragments were cut into small pieces with scissors and placed in vials containing H₂O₂ (2 ml/cm of gel). The vials were capped firmly and incubated overnight at 70°C. Following this, 2 ml aliquots were transferred to fresh scintillation vials (Wheaton, USA), 8 ml scintillation fluid was added and the samples were subjected to liquid scintillation counting in a Beckman LS 6500 liquid scintillation counter (Beckman, USA). The expression of MME and angiostatin (dilution 1:250, rabbit anti-mouse plasminogen, 1-4 Kringle, Abcam, Cambridge, UK and dilution 1:500, mouse monoclonal anti-tubulin, Santa Cruz, USA) in tumor tissue was detected by Western blot analysis as above. The bands observed were compared with the results of the γ -ray analysis.

Immunohistochemistry and immunofluorescence analysis. The antibodies used included a goat polyclonal antibody specific for mouse MME (dilution 1:100, Santa Cruz, CA, USA), a goat polyclonal antibody directed against mouse CD34 (dilution 1:150, Santa Cruz), a rabbit polyclonal antibody for mouse vascular endothelial growth factor (VEGF, dilution 1:200, Santa Cruz), a biotinylated rabbit anti-goat IgG (Boster Biotech, P.R. China) and an Alexa Fluor 568 anti-rabbit IgG (H+L, Invitrogen). The degree of immunostaining for MME was considered positive when unequivocal brown staining of the cytoplasm was observed in CT-26 tumor cells. The microvessel density (MVD) was counted as previously described (17). Several field images of immunofluorescent staining VEGF in the tumor tissue section were captured under a fluorescence inverted microscope (Olympus, Japan). The fluorescence intensity of each section in the images was measured using the Image-Pro Express image analysis software (Media Cybernetic, USA). The mean fluorescence intensity in each section was then calculated.

Statistical analysis. All data were analyzed using the SPSS statistical package (version 12.0 for Windows, SPSS, USA). The data were represented as mean \pm SEM, and the differences among the groups were analyzed using Student's unpaired two-tailed t-test. Categorical variable data were analyzed using the Chi-square test. P<0.05 was considered statistically significant.

Results

Identification and transfection of the recombinant plasmid. As illustrated in Fig. 1A, the MME cDNA fragment was inserted into the expression vector pEGFP-C1, and pEGFP-C1-MME was identified by *Bam*HI and *Xba*I digestion. Direct DNA sequencing showed three base changes in the MME cDNA fragment. Two of these three mutations were in domain I and the other was in domain II.

The recombinant plasmid pEGFP-C1-MME and vector alone (pEGFP-C1) were transfected into CT-26 colon cancer cells. Stable transfectants were selected by G418. After transfection with the pEGFP-C1 vector and pEGFP-C1-MME, GFP expression was observed under fluorescent microscopy. The

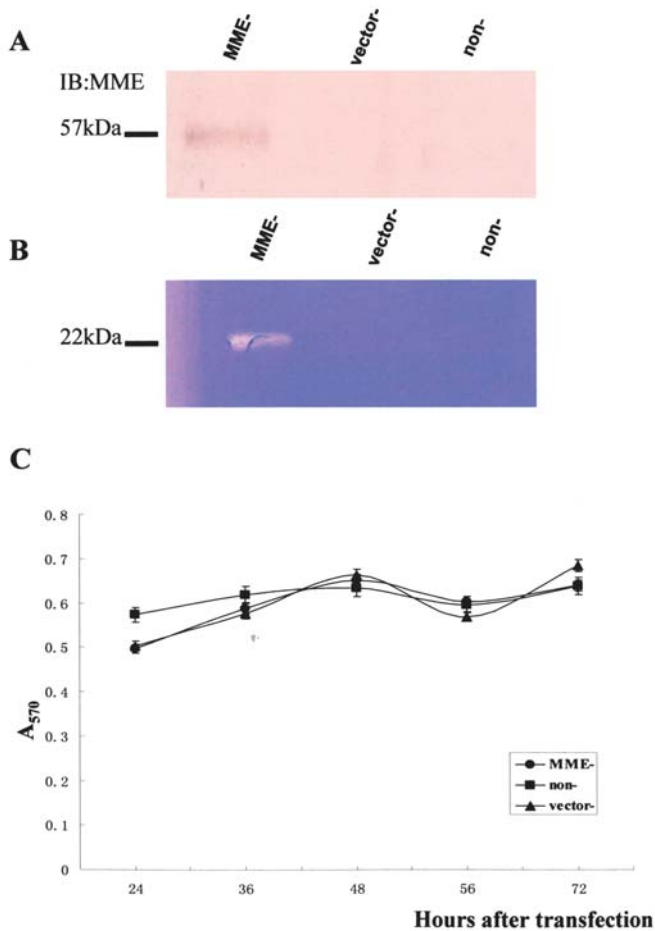


Figure 2. Expression and activity identification of MME in murine CT-26 colon cancer cells and its effect on cell viability. (A) Western blot analysis of the expression of pEGFP-C1-MME (40 μ g of total protein/lane). Lane 1: pEGFP-C1-MME-transfected, lane 2: vector-transfected and lane 3: non-transfected cells. A 57-kDa band was detected in pEGFP-C1-MME transfected cells, but not in vector- and non-transfected cells. The protein with a 57 kDa molecular mass corresponded to domains I and II of MME and GFP. (B) Gelatin zymography analysis. Lane 1: the supernatant of lysed pEGFP-C1-MME-transfected, lane 2: the supernatants of lysed vector-transfected and lane 3: the supernatants of lysed non-transfected cells. A 22-kDa lytic band was identified in pEGFP-C1-MME-transfected cells, whereas no zones of lysis were indicated in the controls. (C) Effects of MME transfection on CT-26 cell growth. MTT analysis shows no obvious growth inhibitory effects in MME-transfected cells compared with the control groups in 72 h ($n>0.05$).

pattern of intracellular GFP distribution appeared differently: GFP in control vector-transfected cells spread throughout the cells (Fig. 1B), whereas GFP in pEGFP-C1-MME-transfected cells was mainly localized in the cytosol (Fig. 1B).

Expression and elastase activity of MME in stably transfected murine CT-26 colon cancer cells. To validate the presence of the MME protein in pEGFP-C1-MME-transfected cells, the conditioned medium from cells growing in serum-free medium was analyzed by Western blot analysis. As shown in Fig. 2A, a 57-kDa band, corresponding to domains I and II plus GFP, was detected in MME-transfected cells, but not in vector- or non-transfected cells.

To determine whether the three base mutations in the recombinant MME altered their proteolytic activity, gelatin

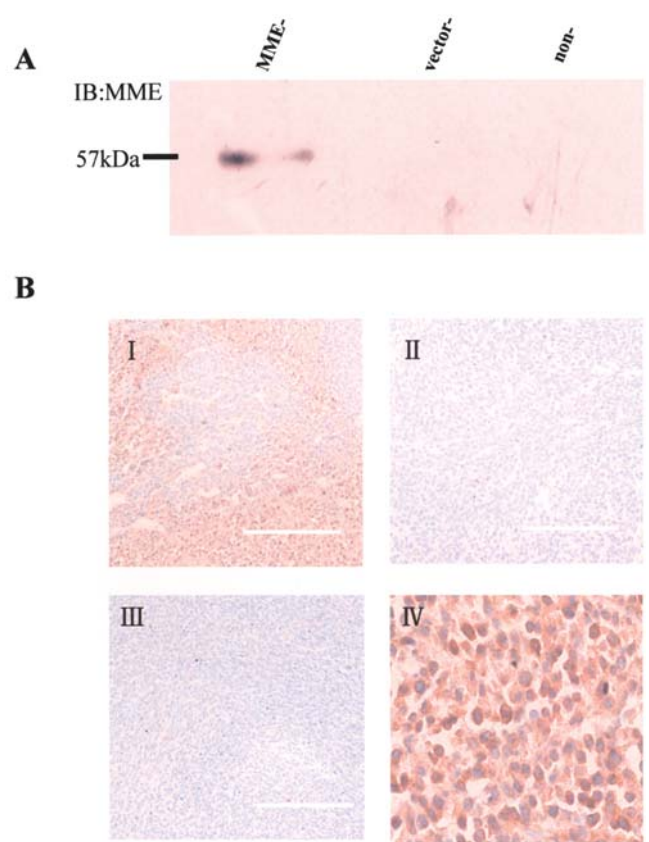


Figure 3. Expression of MME protein in murine colon cancer tissue. (A) Western blot analysis of MME expression. Lane 1: MME-transfected, lane 2: vector-transfected and lane 3: non-transfected groups. A 57-kDa band corresponding to mouse MME was detected in lane 1. (B) Immunohistochemical analysis of MME expression. I: MME-transfected, II: vector-transfected and III: non-transfected tumors. Positive cells were detected in the MME-transfected tumor. No positive cells were detected in the control tumors. Original magnification, $\times 100$; bar inset, 200 μ m. IV: recombinant MME protein displayed a secretory expression in cytoplasm; original magnification, $\times 400$.

zymography was performed. As shown in Fig. 2B, a 22-kDa lytic band was detected only in MME-transfected cells but not in the controls (vector- and non-transfected cells). The 22-kDa band corresponded to the final active form of MME after the cleavage of domain I (8 kDa) and GFP (27 kDa). As shown in Fig. 2C, the expression of recombinant MME did not cause growth inhibitory effects on CT-26 cells.

Expression of MME in a subcutaneously implanted tumor model. Western blot analysis and immunohistochemistry were performed to evaluate MME expression in colon tumor tissues. On Western blot analysis, a 57-kDa MME protein band was present in the MME-transfected tumor tissue, whereas no band was observed in the vector- and non-transfected tumor tissues (Fig. 3A). A high level of MME expression in the MME-transfected tumors was demonstrated by immunohistochemistry. The non- and vector-transfected groups showed no significant expression of MME (Fig. 3B).

Overexpression of MME inhibits subcutaneous tumor growth in mice. To determine whether the forced expression of recombinant MME altered the tumorigenicity of CT-26 in

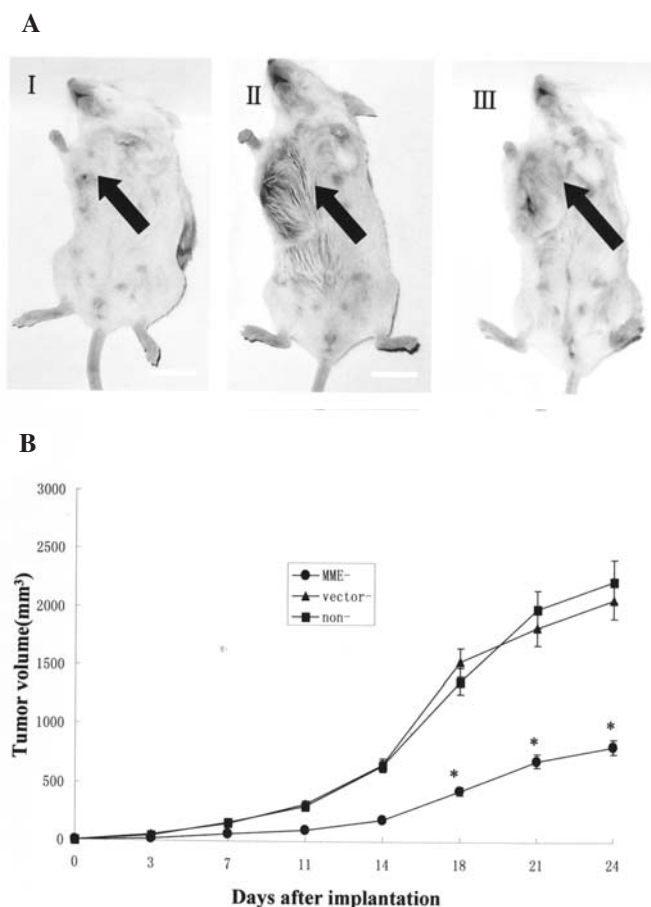


Figure 4. Suppression of murine colon cancer growth. (A) Macroscopic characteristics of the tumors are shown 4 weeks after implantation. Tumors derived from the MME- and vector-transfected clones, and the non-transfected CT-26 parental cells were measured. I: MME-transfected, II: vector-transfected and III: non-transfected groups. The tumor location is shown by the black arrows; bar inset, 1.5 cm. (B) *In vivo* growth rate of subcutaneous tumors derived from the MME-transfected and vector-transfected clones, and the non-transfected parental cells. Tumor volumes were determined at several time points using the formula: smallest diameter x widest diameter/2 and all values are represented as mean \pm SEM (n=30 mice/group). At 4 weeks, mice carrying non- or vector-transfected cells formed large tumors with volumes of >2000 mm³. In contrast, mice implanted with MME-transfected cells significantly formed smaller tumors (616.04 ± 121.33). *P<0.001, by Student's unpaired two-tailed t-test.

mice, the control and MME-transfected cells were inoculated into the subcutis of syngeneic mice. Tumor volumes were determined 4 weeks after the inoculation. Representative results are shown in Fig. 4A. The vector- and non-transfected cells formed large subcutaneous tumors with volumes of 2071.80 ± 608.96 and 2231.90 ± 496.91 mm³ 4 weeks after implantation, respectively. In contrast, MME-transfected cells formed smaller tumors, with volumes of 816.56 ± 234.02 mm³. Therefore, the growth of MME-transfected tumors was significantly retarded compared with the control tumors (P<0.001). There was no significant difference between the control groups (Fig. 4B). Forty-six out of 60 mice (76.6%) in the control groups developed thoracic cavity metastases, but only 11 out of 30 mice (36.6%) with thoracic cavity metastases were found in the MME-transfected group. No liver metastasis was found in any mouse in the three groups. There was a

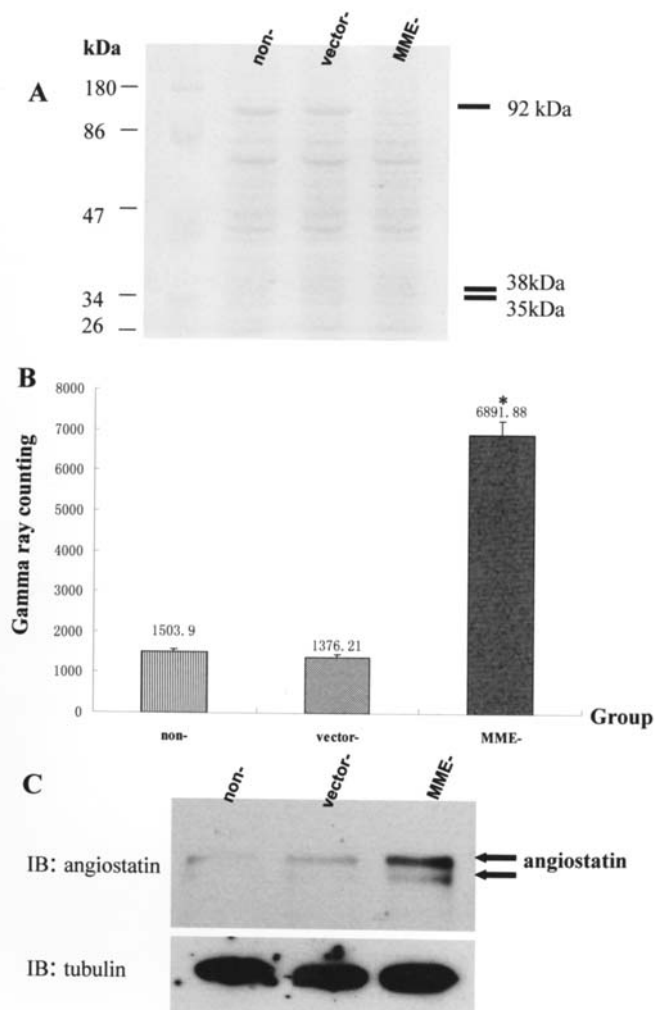


Figure 5. Detection of mouse angiostatin in tumor tissue. (A) SDS-PAGE electrophoresis. Lane 1: prestain marker, lane 2: non-transfected, lane 3: vector-transfected and lane 4: MME-transfected groups. The positions of plasminogen (92 kDa) and angiostatin (38 kDa, 1-4 Kringle and 35 kDa, 1-3 Kringle) are shown (black arrows). (B) The γ -ray counting analysis for radioactivity in the gel. The values are represented as mean \pm SEM of radioactivity per areas which contained the protein with a molecular weight of 35 and 38 kDa. They were significantly higher in the amount of radioactivity detected in the MME-transfected group than the control groups. *MME-transfected versus the non- or vector-transfected groups; P<0.01, by Student's unpaired two-tailed t-test. (C) Western blot analysis of the angiostatin generation in tumor tissues. Protein (40 μ g) per lane from tumor tissues were separated by 12% SDS-PAGE, blotted and probed using a specific anti-mouse plasminogen (1-4 Kringle) antibody. Lane 1: non-transfected, lane 2: vector-transfected and lane 3: MME-transfected groups. Two bands (35 and 38 kDa, black arrows) corresponding to the mouse angiostatin were identified. Quantification of the protein signals by image analysis revealed that the angiostatin protein levels were significantly increased in MME-transfected tumor tissues compared with the control groups, P<0.01.

statistically significant difference in the survival period of the MME-transfected group (1 out of 30 mice died within 4 weeks) and the control groups (6 and 8 out of 30 mice died within 4 weeks in the vector- and non-transfected groups, respectively, P<0.05).

MME is an enzyme for the angiostatin generation in vivo. To identify the role of MME in the generation of angiostatin *in vivo*, SDS-PAGE and γ -ray counting analysis were used to

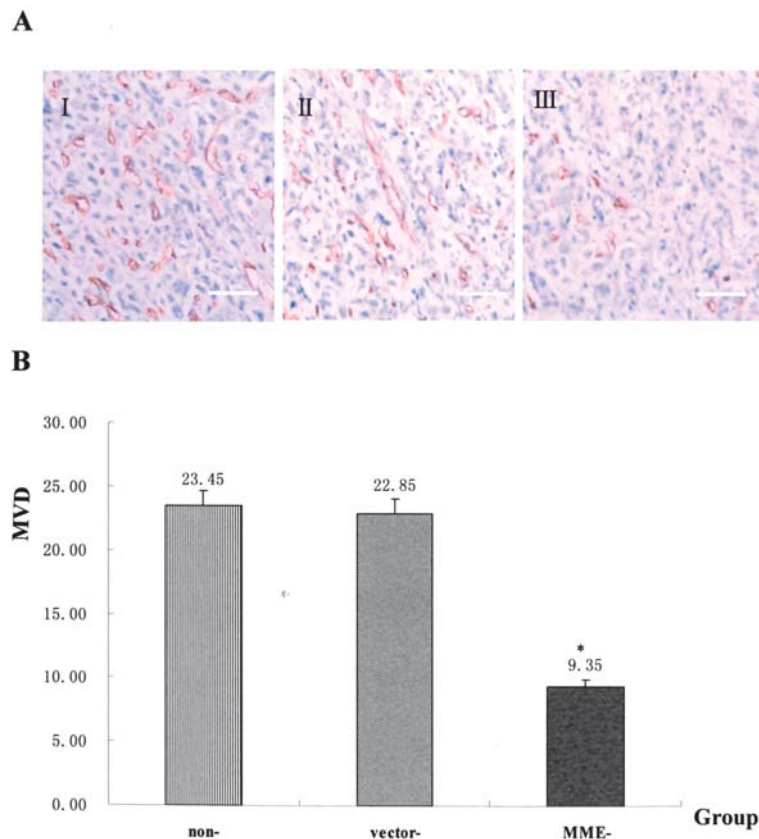


Figure 6. Microvessel density of subcutaneously implanted tumors. (A) Staining with polyclonal antibody against mouse CD34. Immunohistochemistry of the vascularization of subcutaneously implanted tumors was performed. I-III: representative sections showing neovascularization in tumor tissues, I: non-transfected, II: vector-transfected and III: MME-transfected groups; original magnification, $\times 200$; bar inset, $200 \mu\text{m}$. (B) MVD was counted from five different high-power fields, and the values are represented as mean \pm SEM. Tumors derived from MME-transfected cells demonstrated a lower microvessel density compared with the two control groups. * $P < 0.001$, by Student's unpaired two-tailed t-test.

detect the size of the radioactive band and the radioactive intensity in the tumor tissue. Western blot analysis was used to assay the expression of angiostatin in the samples for comparison. Data show that the SDS-PAGE gel contained the protein with molecular weights of 35 and 38 kDa (Fig. 5A), and that the radioactivity of the MME-transfected group (6891.88 ± 768.86) was significantly higher than the control group (Fig. 5B). The radioactivity of the non-transfected and vector groups was 1503.9 ± 304.42 and 1376.21 ± 186.36 , respectively. In the Western blot analysis, we also detected the generation of angiostatin in the MME-transfected group (Fig. 5C). In contrast, the control group showed two very faint bands for angiostatin (Fig. 5C). Quantification of the protein signals revealed that the angiostatin protein levels increased (9.32 ± 1.52 and 5.61 ± 2.24) in the MME-transfected tumor tissues, compared with the vector-transfected (2.47 ± 0.23 and 0.67 ± 0.12) and non-transfected tumor tissues (1.21 ± 0.69 and 0.86 ± 0.44), $P < 0.01$.

Microvessel density of the subcutaneously implanted tumors. Immunohistochemistry of the vascularization of subcutaneously implanted tumors was performed by staining with a polyclonal antibody against mouse CD34 (Fig. 6A). Tumors derived from MME-transfected cells demonstrated a lower microvessel density (9.35 ± 2.79) compared with control tumors derived from vector-transfected (22.85 ± 3.80) and non-

transfected (23.45 ± 4.49) cells (Fig. 6B, MME versus vector and parental at $P < 0.001$ and $P < 0.001$, respectively). There was no significant difference between the two control groups.

Expression of VEGF in the subcutaneously implanted tumor model. Immunofluorescence detected the VEGF expression mainly in colon cancer cells in the central and marginal areas of the tumor tissue (Fig. 7A). The non-neoplastic colon cells showed no signal or a weak fluorescence intensity. No significant fluorescence was seen in the sections that were used at the same time as a negative control. The fluorescence intensity levels of VEGF in tumor cells were significantly lower in the MME-transfected group (20.16 ± 7.32) than in the control groups ($P < 0.01$). There was no significant difference between the vector-transfected (60.51 ± 15.19) and non-transfected (61.60 ± 17.90) groups (Fig. 7B).

Discussion

Plasminogen, a single-chain glycoprotein of 92 kDa consisting of an N-terminal peptide, five kringle domains and a serine protease domain (18), play a crucial role in tumor metastasis and angiogenesis where localized proteolysis is required. Under certain conditions, plasminogen undergoes proteolysis to form kringle-containing A-chain fragments, collectively called angiostatins (19-21), which are novel and potent

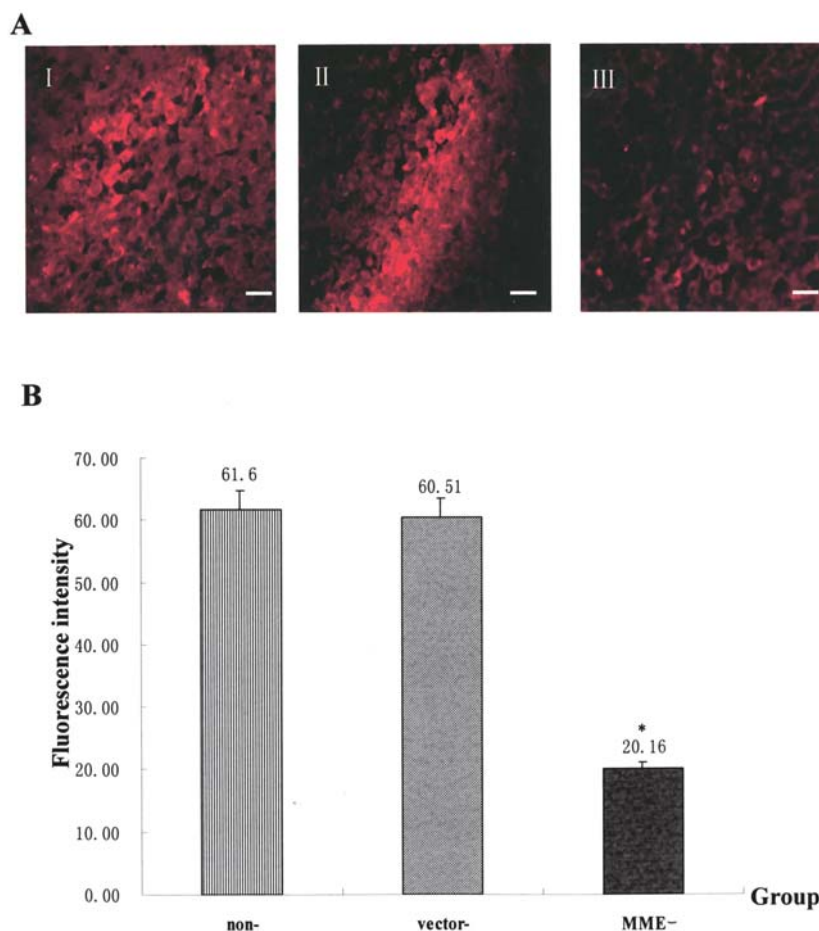


Figure 7. VEGF expression in subcutaneously implanted tumors. (A) Expression of VEGF was confirmed by the presence of fluorescence-stained cytoplasm in the tumor cells. I: non-transfected, II: vector-transfected and III: MME-transfected groups; original magnification, x400; bar inset, 40 μ m. The weaker fluorescence intensity expression was observed in the tumor of the MME-transfected group. (B) Fluorescence intensity was measured from the tumor tissue section, and the values are represented as mean \pm SEM. The fluorescence intensity levels of VEGF in tumor cells were significantly lower in the MME-transfected groups than in the control group. * $P < 0.01$, by Student's unpaired two-tailed t-test.

inhibitors of endothelial cell proliferation and tumor angiogenesis (22). Typically, angiostatin consists of the first four kringle domains (K1-4). The cleavage of plasminogen is performed by proteinases, such as matrix metalloproteinases that are derived from tumor cells or infiltrating macrophages (23,24). These kringle domains and their relatives inhibit the proliferation of vascular endothelial cells, a fundamental process in angiogenesis (20). O'Reilly *et al* (19) first reported that primary tumors may limit metastatic growth by the generation of anti-angiogenic agents. Dong *et al* (25) further demonstrated that macrophage-derived metalloelastase was associated with the production of anti-angiogenic activity by tumors.

MME has been associated with the generation of angiostatin in a murine model of Lewis lung carcinoma (22). Although an MME activity, sufficient to cleave plasminogen to angiostatin, has been demonstrated in a serum-free conditioned medium of carcinoma cells (26), the MME-dependent mechanism of the angiostatin generation *in vivo* remains elusive. The few published studies of human tumor tissue or animal models (6,27) did not confirm directly that the observed increase of angiostatin was due to the cleavage of plasminogen by MME.

In the present study, we successfully constructed the mammalian cell expression plasmid pEGFP-C1-MME, and expressed the recombinant MME in CT-26 murine colon cancer cells. Based on the location of green fluorescence from GFP of the fusion protein, we concluded that MME was distributed evenly in the cytoplasm (Fig. 1). This finding is in agreement with the result of immunohistochemistry staining in tumors formed by pEGFP-C1-MME-transfected cells (Fig. 3). Recombinant MME protein was also detected by Western blot analysis in the MME-transfected cells (Fig. 2), and it showed a secretory expression in the tumor tissue on immunohistochemistry (Fig. 3). These results suggest that secretion of the recombinant pEGFP-C1-MME protein can occur *in vivo*.

To determine whether the recombinant MME was able to generate angiostatin in tumors, we investigated the catabolism of radio-labeled plasminogen. The γ -ray counting data demonstrated that plasminogen cleavage occurred mostly in tumors formed by cells forced to express (Fig. 5). Plasminogen cleavage by MME generates 38 kDa (angiostatin K1-4) and 35 kDa (angiostatin K1-3) fragments with radioactivity. MME-deficient groups were feeble and incapable of the degradation of plasminogen to angiostatin (Fig. 5). Although other

components may participate in the generation of angiostatin *in vivo*, the localization of high levels of angiostatin in tumors derived from MME-transfected clones (Fig. 5) illustrate, without doubt, the important role of MME in anti-angiogenesis mediated by angiostatin. These data not only support the idea that the production of angiostatin mainly depends on the biological activity of MME, but also agree with a previous report that the MME released directly from the MME-transfected tumor cells most likely cleaves the circulating plasminogen sequestered in the tumor stroma into active angiostatin (5).

Our results provide further experimental evidence that the forced expression of MME significantly inhibits the growth of CT-26 tumors in mice (Fig. 4). An analysis of the tumor MVD by staining with CD34 antibody confirmed that MME-transfected tumors showed a lower MVD compared with the controls (Fig. 6). Moreover, we demonstrated that the level of VEGF protein expression in MME-transfected tumors was significantly lower than that in the controls (Fig. 7). These data suggest that the suppression of tumor cells in mice by MME was caused by the inhibition of angiogenesis in the tumor lesions, possibly due to the generation of angiostatin by MME.

In conclusion, we successfully constructed the vector, pEGFP-C1-MME and transfected the MME gene into murine colon cancer cells. In addition, the biological properties of MME, plasminogen and angiostatin appear to be tightly linked *in vivo*. These data suggest that MME is responsible, at least in part, for the inhibition of tumor angiogenesis in this tumor model.

Acknowledgements

This work was supported by the Department of Technology Natural Science Foundation of Anhui province grant 01043904 and the Department of Education Natural Science Foundation of Anhui province grant 2003 KG199. We sincerely thank The Key Laboratory of Gene Resource Utilization for Genetic Diseases, Ministry of Education and Anhui Province, especially M. Stanciu, M. Hai Ping Wang and Lijie Feng.

References

- DeClerck YA, Mercurio AM, Stack MS, *et al*: Proteases, extracellular matrix, and cancer: a workshop of the path B study section. *Am J Pathol* 164: 1131-1139, 2004.
- Burg-Roderfeld M, Roderfeld M, Wagner S, *et al*: MMP-9-hemopexin domain hampers adhesion and migration of colorectal cancer cells. *Int J Oncol* 30: 985-992, 2007.
- Werb Z and Gordon S: Elastase secretion by stimulated macrophages. Characterization and regulation. *J Exp Med* 142: 361-377, 1975.
- Fu JY, Lyga A, Shi H, Blue ML, Dixon B and Chen D: Cloning, expression, purification, and characterization of rat MME. *Protein Expr Purif* 21: 268-274, 2001.
- Gorin-Rivas MJ, Arie S, Furutani M, *et al*: Mouse macrophage metalloelastase gene transfer into a murine melanoma suppresses primary tumor growth by halting angiogenesis. *Clin Cancer Res* 6: 1647-1654, 2000.
- Dong Z, Kumar R, Yang X and Fidler IJ: Macrophage-derived metalloelastase is responsible for the generation of angiostatin in Lewis lung carcinoma. *Cell* 88: 801-810, 1997.
- Gorin-Rivas MJ, Arie S, Mori A, *et al*: Implications of human macrophage metalloelastase and vascular endothelial growth factor gene expression in angiogenesis of hepatocellular carcinoma. *Ann Surg* 231: 67-73, 2000.
- Kerkela E, Ala-Aho R, Jeskanen L, *et al*: Expression of human macrophage metalloelastase (MME) by tumor cells in skin cancer. *J Invest Dermatol* 114: 1113-1119, 2000.
- Hofmann HS, Hansen G, Richter G, *et al*: Matrix metalloproteinase-12 expression correlates with local recurrence and metastatic disease in non-small cell lung cancer patients. *Clin Cancer Res* 11: 1086-1092, 2005.
- Shi H, Xu JM, Hu NZ, Wang XL, Mei Q and Song YL: Transfection of mouse macrophage metalloelastase gene into murine CT-26 colon cancer cells suppresses orthotopic tumor growth, angiogenesis and vascular endothelial growth factor expression. *Cancer Lett* 233: 139-150, 2006.
- Shen YX, Ballar P and Fang SY: Ubiquitin ligase gp78 increases solubility and facilitates degradation of the Z variant of a-1-antitrypsin. *Biochem Biophys Res Commun* 349: 1285-1293, 2006.
- Yoshimoto M, Kinuya S, Kawashima A, Nishii R, Yokoyama K and Kawai K: Radiiodinated VEGF to image tumor angiogenesis in a LS180 tumor xenograft model. *Nucl Med Biol* 33: 963-969, 2006.
- Wachsberger PR, Burd R, Marero N, *et al*: Effect of the tumor vascular-damaging agent, ZD6126, on the radioresponse of U87 glioblastoma. *Clin Cancer Res* 11: 835-842, 2005.
- Takeda Y: Plasminogen-125 I responses in dogs to a single injection of urokinase and typhoid vaccine and to vascular injury. *J Clin Invest* 51: 1363-1377, 1972.
- Lee KH, Song SH, Paik JY, Byun SS, *et al*: Specific endothelial binding and tumor uptake of radiolabeled angiostatin. *Eur J Nucl Med Mol Imaging* 30: 1032-1037, 2003.
- Zhou S, Bailey MJ, Dunn MJ, Preedy VR and Emery PW: A systematic investigation into the recovery of radioactively labeled proteins from sodium dodecyl sulfate-polyacrylamide gels. *Electrophoresis* 25: 1-7, 2004.
- Shi H, Xu JM, Hu NZ and Xie HJ: Prognostic significance of expression of cyclooxygenase-2 and vascular endothelial growth factor in human gastric carcinoma. *World J Gastroenterol* 9: 1421-1426, 2003.
- Forsgren M, Raden B, Israelsson M, Larsson K and Heden LO: Molecular cloning and characterization of a full-length cDNA clone for human plasminogen. *FEBS Lett* 213: 254-260, 1987.
- O'Reilly MS, Holmgren L, Shing Y, *et al*: Angiostatin: a novel angiogenesis inhibitor that mediates the suppression of metastases by a Lewis lung carcinoma. *Cell* 79: 315-328, 1994.
- Kassam G, Kwon M, Yoon CS, *et al*: Purification and characterization of A61. An angiostatin-like plasminogen fragment produced by plasmin autodigestion in the absence of sulfhydryl donors. *J Biol Chem* 276: 8924-8933, 2001.
- Kwon M, Yoon CS, Fitzpatrick S, *et al*: p22 is a novel plasminogen fragment with antiangiogenic activity. *Biochemistry*. *Biochemistry* 40: 13246-13253, 2001.
- Cornelius LA, Nehring LC, Harding E, *et al*: Matrix metalloproteinases generate angiostatin: effects on neovascularization. *J Immunol* 161: 6845-6852, 1998.
- Morikawa W, Yamamoto K, Ishikawa S, *et al*: Angiostatin generation by cathepsin D secreted by human prostate carcinoma cells. *J Biol Chem* 275: 38912-38920, 2000.
- Lay AJ, Jiang XM, Kisker O, *et al*: Phosphoglycerate kinase acts in tumour angiogenesis as a disulphide reductase. *Nature* 408: 869-873, 2000.
- Dong Z, Yoneda J, Kumar R and Fidler IJ: Angiostatin-mediated suppression of cancer metastases by primary neoplasms engineered to produce granulocyte/macrophage colony-stimulating factor. *J Exp Med* 188: 755-763, 1998.
- Gately S, Twardowski P, Stack MS, *et al*: Human prostate carcinoma cells express enzymatic activity that converts human plasminogen to the angiogenesis inhibitor, angiostatin. *Cancer Res* 56: 4887-4890, 1996.
- Shapiro SD, Griffin GL, Gilbert DJ, *et al*: Molecular cloning, chromosomal localization, and bacterial expression of a murine macrophage metalloelastase. *J Biol Chem* 267: 4664-4671, 1992.